

CAOS Smart Camera-based Robust Low Contrast Image Recovery over 90 dB Scene Linear Dynamic Range

Nabeel. A. Riza and Mohsin. A. Mazhar; School of Engineering, University College Cork; Cork, Ireland

Abstract

Experimentally demonstrated for the first time is Coded Access Optical Sensor (CAOS) camera empowered robust and true white light High Dynamic Range (HDR) scene low contrast target image recovery over the full linear dynamic range. The 90 dB linear HDR scene uses a 16 element custom designed test target with low contrast 6 dB step scaled irradiances. Such camera performance is highly sought after in catastrophic failure avoidance mission critical HDR scenarios with embedded low contrast targets.

Introduction

It is well known that both natural and human-made scenes can have critical optical information distributed across different irradiance bands within the full HDR of the irradiance data [1]. Specifically, these critical irradiance values within a specific sub-range of the full irradiance map can display low image contrast. In order for robust and true image contrast recovery over the full HDR of a camera imaged scene, required is a linear Camera Response Function (CRF), i.e., input-output system response over the entire HDR. Considering linear HDR values of ≥ 90 dB, highly deployed commercial CMOS [2-7], CCD [8-9] and FPA (Focal Plane Array) [10] based image sensors are hard pressed to deliver robust and true irradiance maps under low contrast conditions over a full HDR. A fundamental reason for this limitation is the difficulty in designing and physically realizing in hardware a high linearity, uniform sensitivity, and adequate Signal-to-Noise Ratio (SNR) multi-pixel optical sensor opto-electronic array device over the full HDR [11]. Indeed, recent experiments conducted with an up-to 87 dB HDR commercial CMOS sensor camera from Thorlabs has shown limitations in recovery of robust true linear HDR image data [12]. To provide an update on HDR CMOS sensor technology, Table 1 shows recent CMOS sensor HDR numbers and their HDR generation methods listed by some vendors.

As proposed recently, CAOS is an alternate way to design an optical camera based on the principles of multiple access RF/optical wireless networks [12-14]. The origins of the CAOS camera and its forerunner, the agile pixel imager, in the context of prior art is described in ref.15 and ref.16 [15-16]. The seeds of the CAOS invention were laid in 1985 when N. A. Riza as a MS/PhD student at Caltech attended the legendary physics Nobel laureate Professor Richard P. Feynman's class (see Fig.1). Professor Feynman basically said: There is Radio Moscow in this room, there is Radio Beijing in this room, there is Radio Mexico city in this room; then he paused and said: aren't we humans fortunate that we can't sense all these signals; if we did we would surely go mad with the massive overload of electromagnetic radiation (radio signals) around us! These words of wisdom led to the CAOS invention as even today, radio signals are all around us, each encoded with their unique Radio Frequency (RF) signatures. So when one desires, one can "hear" these RF signals if one uses the correct time-frequency codes to decode these super weak signals using coherent electronic signal processing via sensitive RF receivers. In fact, this encode-decode operation happens in today's RF mobile cellular phone network where each mobile user has a specific assigned code, i.e., telephone number. Many users simultaneously use the RF spectrum and multiple access techniques are used to acquire the desired signals. One can apply the same principles of a multi-access multiple user RF network to the optical imaging task where one can treat optical pixels in the image space as independent mobile users assigned specific telephone codes using a

2-D time-frequency optical array modulating device. Next an optical antenna (i.e., lens) can be used to catch all these time-frequency encoded optical signals/pixel data set that is converted to an AC signal by a sensitive optical-to-electrical converter, e.g., high speed point photo-detector with an amplifier. This AC signal is subjected to sensitive AC-style (in Hz domain vs DC domain) electronic Digital Signal Processing (DSP) for decoding pixel data, including using multiple access decoding methods for simultaneous pixels detection. By doing so, many optical pixels can be observed with extremely high linear Dynamic Range (DR) and SNR control, realizing the CAOS camera. Combined with classic multi-pixel optical sensors that detect DC (i.e., unmodulated) light maps, one forms the CAOS smart camera that inherently also makes a fault-tolerant robust camera system with full spectrum capabilities and extremely secure operations.

Table 1: Example Commercial HDR Silicon CMOS Sensors.

Company	HDR Method	Range
New Imaging Technologies (France) 2016	Log Compression	140 dB
Analog Devices (USA) 2017	Log Compression	130 dB
Photonfocus (Swiss) 2016	Linear	60 dB
	Log Compression	60 to 120 dB
Omnivision (USA) 2016	Linear (Deep QW)	94 dB
	Double Exposure	94 to 120 dB
ON-Semi USA (2018)	Linear (1 exposure)	95 dB
	4 Exposures	140 dB
Melexis-Cypress-Sensata (USA) 2017	Piece-wise Linear (Non-linear) (Multi-Slope using Pixel Resets)	150 dB

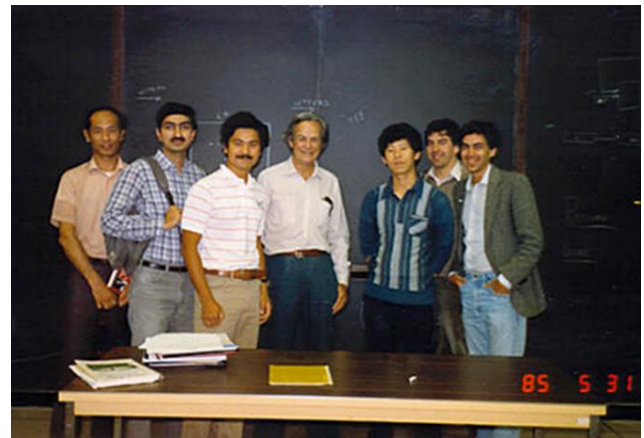


Figure 1. Shown is Prof. Richard P. Feynman (centre), 1965 Physics Nobel Prize, in his 1985 graduate class at Caltech where Prof. Feynman's words many years later inspired N. A. Riza (2nd from left) to invent the CAOS camera.

There is also another similarity between CAOS and the RF wireless multi-access mobile phone network, i.e., both operate with an intrinsic HDR design. Fig.2 shows key design parameters of the RF network one cell zone with a radius of d_1 . Mobile users are labelled as $M_1, M_2, M_3, \dots, M_n$, where n is the mobile user's number. The n^{th} mobile user M_n is located at a distance d_n from the cell base station antenna that transmits P_T dBm radiated RF power with all user communication channels within its coded bandwidth. The n^{th} mobile RF receiver harvests P_n RF power that drops as d_n increases for users farther from the base station antenna. There are various standards for which the RF network is design. For example, for the GSM network standard, the minimum detectable RF signal power at the mobile receiver is -102 dBm [17]. For the example in Fig.2, the M_1 user is farthest from the base station antenna, hence $P_1 = -102$ dBm. Transmitted RF power P_T from base station antenna can be as high as 43 dBm for suburban or rural areas [17], which implies that the ratio between the transmitted RF power and minimum received RF power is $102+43=145$ dB, indeed a HDR. In other words, the RF network is designed for HDR operations within a cell as users can be very close to the base station antenna as well as on the boundary of the cell zone. Hence, the received RF power radiation map of all users covers a HDR, much like the HDR optical image map captured by CAOS using the principles of a RF multi-user wireless phone network. There-in is showcased the similarity between an HDR optical image pixel caught by the CAOS camera and the HDR RF radiation power caught by the mobile user's RF receiver.

Also, the CAOS smart camera design in one sense follows nature's human eye rods and cones dual photo-cells design as the CAOS smart camera features image fusion to produce optimized (i.e., linear response and adequate SNR) imaging using CAOS pixels and CMOS/CCD/FPA pixels. It has also been shown that the CAOS camera intrinsically is a linear camera response highly programmable smart camera that so far has reached a 177 dB linear Extreme Dynamic Range (EDR) [12]. Given CAOS's linear CRF feature, it is naturally suited for low contrast image recovery over an EDR. Given this low contrast image detection capability that can be critical for many applications such as search and rescue, medical imaging, industrial parts inspection and still photography, the present paper for the first time experimentally demonstrates the low contrast image recovery capability of the CAOS camera over a scene instantaneous EDR.

Fig.3 highlights the design of the CAOS smart camera using key components such as the TI Digital Micromirror Device (DMD), point Photo-Detector Module (PD-M), point Photo-Multiplier Tube Module (PMT-M), lenses (L), shutter (S), aperture (A1), CMOS sensor, Mirror-Motion Module (MM-M), and Variable Optical Attenuators (VOAs). The DMD acts as the required space-time-frequency optical coding device to generate the wireless style CAOS signals required for linear HDR imaging via high speed Digital Signal Processing (DSP). For example, Pixels of Interest (POI) in the image incident on the DMD plane in the CAOS camera can be simultaneously encoded with orthogonal time sequences such as Walsh codes and the combined light from the POI is next captured by a pair of point optical antennas (i.e., high speed point detectors) that generate AC signals that are sampled by a pair of Analog-to-Digital Converters (ADCs). This encoding method is called Code Division Multiple Access (CDMA), a terminology from RF Wireless. The digitized AC signals carrying the coded POI data undergo time-frequency correlation-based decoding via DSP to recover the selected POI image. The POI coding can also include Frequency Modulation (FM) encoding of the incident imaged light so pixel irradiance data are present on an RF carrier (e.g., 25 KHz) that enables low 1/f noise HDR decoding via DSP-based RF spectrum analysis. Parallel, time sequential, and combined Parallel-Time sequential POI encoding and decoding can be implemented in CAOS based on the imaging requirements. Further details of the CAOS camera design and its advanced modes of operation similar to a RF wireless multi-access network are described in detail in an earlier publication [18].

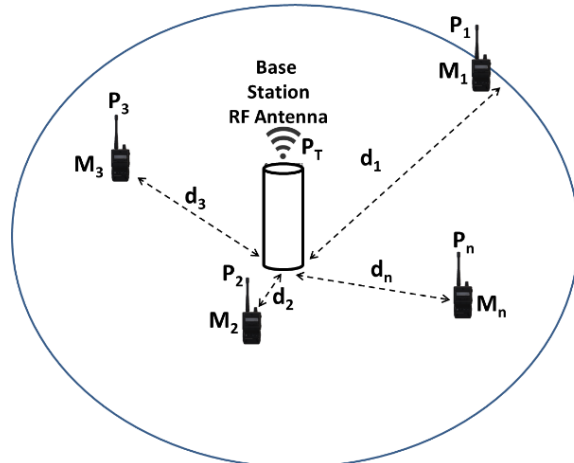


Figure 2. Shown is the RF Wireless Multi-Access Mobile Phone Network operations within one Cell zone. Both CAOS and the RF Network operate with an intrinsic HDR design.

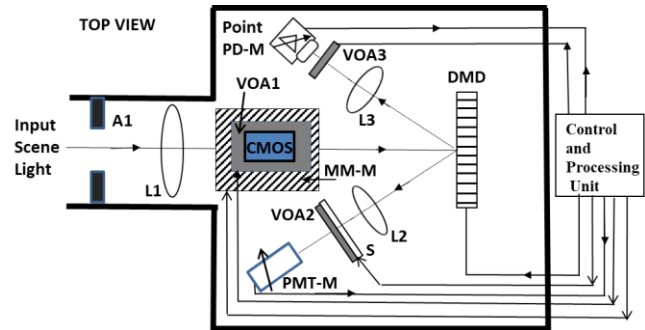


Figure 3. Shown is the top view of the CAOS smart camera [12].

To test low contrast image recovery over a HDR, one requires a low contrast resolution HDR chart (e.g., see Fig.4) that has pairs of image patches in the HDR scene that have 2:1 relative irradiance values across the entire test HDR [19]. A 2:1 relative irradiance step between two adjacent patches gives a 6 dB DR step between the two test patches. In other words, for effective low contrast image recovery of an HDR scene, the camera must be able to correctly measure all the irradiance value 6 dB DR steps across the full HDR. To experimentally test the CAOS camera's low contrast recovery capability versus a standard commercial CMOS sensor's performance, a 90 dB HDR chart with 16 patches is built using commercial Neutral Density (ND) optical filters whose Thorlabs specified attenuation ratings are experimentally verified in the laboratory using a precision Newport power meter and stable laser source. Fig.4 shows the in-house designed and verified DR values for each target patch, showing the designed relative 6 dB step. The 0 dB DR patch corresponds to the clear patch that provides the brightest patch in the scene. The inter-patch region is a black acetate sheet material that makes this test target of the low glare type [20]. The goal of the experiment is to correctly measure the designed patch DR values using the deployed CAOS smart camera which includes both the CMOS-mode using the CMOS sensor as well as the CAOS mode using the DMD-based CAOS camera.

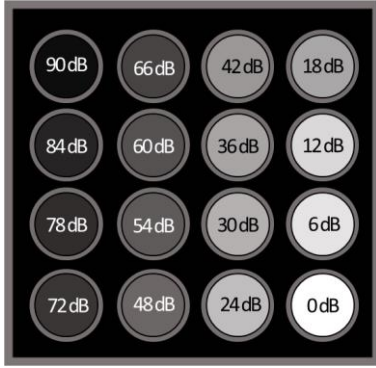


Figure 4. The 90 dB HDR test target scene with low contrast (2:1 relative irradiance) or 6 dB steps in DR across patch pairs over full HDR.

Low Contrast Detection Experiment

The Fig.3 CAOS smart camera is assembled in the laboratory with the test image as follows. The camera system components are: Vialux V-7001 DMD board with a 13.68 μm micro-mirror size, A1 aperture diameter of 9.8 mm, L1 imaging lens Focal Length (FL) of 6 cm, light capture lens L2 FL of 5 cm, visible light Quantalux Thorlabs Model CS2100-M 2.1 Mpixel 1920 x 1080 pixels monochrome silicon s-CMOS sensor with 5.04 microns side square pixel, Image Engineering (Germany) Model LG3 Lightbox white LED light source set to 60 kilo-lux, target scene placed 105 cm from L1, L1 to DMD distance of 6.4 cm, 16 patch target scene assembly of 9.1 cm x 9.1 cm with an inter-patch distance of 1.45 cm with each target patch with a Thorlabs ND filter aperture size of 1.27 cm diameter, National Instruments model USB 6366 DAQ 16-bit analog-to-digital converter, Dell laptop model i7 Latitude 5480 for DSP, and point PMT-M Thorlabs model PMM02.

Given the CAOS smart camera can engage the CMOS sensor, it is natural to first consider the use of multi-exposure HDR recovery methods for the Fig.4 scene capture. Such an approach using leading prior-art multi-exposure HDR algorithms with the deployed s-CMOS sensor from Thorlabs has been reported in detail in ref.21 (a sister paper with the current paper) and the experimentally acquired image data has proven to be inaccurate within the 90 dB full HDR range [21]. Nevertheless, the CMOS-mode of the CAOS smart camera should be used to get a first estimate of the target scene. Hence the Table 2 data is taken as follows.

First the CMOS-mode of the camera is engaged to image the test target without saturating the CMOS sensor which requires setting the CMOS device integration time to 0.414 ms. This CMOS sensor has a specified instantaneous DR of up-to 87 dB with a 16-bit raw image data signal output. Table 2 patch-based CMOS sensor signal values are calculated using the mean of 8100 brightest CMOS pixels within each patch of size 100x100 pixels. The CMOS sensor noise floor is computed using an average of 8100 brightest pixels in a patch of size 100x100 in the imaged region with no light. CMOS-mode measured SNR stays around 2 between the 66 dB to 90 dB patches, enabling spatial registration of even these very weak light patches. In effect, the CMOS sensor is able to spatially identify all 16 patch zones of the 90 dB HDR viewed scene. This SNR>1 data provided by the CMOS sensor provides the required initial scene intelligence that is part of the CAOS smart camera operations. Using this patch spatial data, the Fig.3 camera CAOS-mode is used to obtain robust DR readings for all 16 patches.

Next, three different CAOS modes explained in reference [18] are used for imaging of the 16 patches. Table 2 data with superscripts a, b, c refer to CAOS CDMA, FM TDMA-1 (FM Time Division Multiple Access) high spatial resolution and FM TDMA-2 low spatial resolution modes, respectively. First the CDMA-mode is used that robustly recovers the low contrast patches with DR reaching 54 dB. The CDMA-mode imaged a 63 x 65 CAOS pixels grid with each CAOS

pixel of 6 x 6 micromirrors of the DMD. Each CAOS pixel is encoded with a 4096 bits Walsh sequence in time with bit rate of 1 KHz giving an encoding time of 4.096 sec. Note that a 50X reduction in encoding time is possible if one deploys the 50 KHz bit rate option in the DMD as used in some of our prior work for CAOS POI scene real-time imaging [12]. CAOS CDMA-mode pixel signal scaled irradiance values are calculated using the mean of 36 brightest pixels within each target patch of size 7x7 CAOS pixels. CDMA-mode noise floor is computed using an average of scaled pixel irradiances in a patch of size 7x7 in a region with no light. Table 2 shows the CDMA-mode to be accurate in image recovery up-to the 54 dB DR patch, i.e., 10 patches within the 16 patches target are accurately recovered, leaving 6 patches for CAOS alternate modes recovery.

Table 2. Designed and Measured patch DR values using both the CMOS sensor and the CAOS camera set to its various CAOS modes, i.e., a: CDMA, b: FM TDMA-1 (high resolution) and c: FM TDMA-2 (low resolution).

Design (dB)	CMOS Measured (dB)	CAOS Measured (dB)	CAOS Signal to Noise Ratio
0	0	0 ^a	1065
6	5.39	4.19 ^a	659
12	12.23	10.06 ^a	335
18	18.38	15.53 ^a	178
24	23.38	24.75 ^a	62
30	29.40	28.20 ^a	41
36	32.82	33.09 ^a	23.6
42	40	39.6 ^a	11.2
48	40.6	47.5 ^a	4.5
54	46.71	54.04 ^a	2.1
60	48.34	61.16 ^b	1.5
66	50.64	64.08 ^b	1.1
66	-	64.87 ^c	203
72	50.94	73.4 ^c	78.3
78	51.17	78.94 ^c	43.6
84	51.17	83.29 ^c	24.8
90	50.94	90.1 ^c	11.0

Specifically, chosen is the lower inter-pixel crosstalk FM-TDMA mode for scaled irradiance measurements of the remaining 6 patches whose zones have already been identified by the CMOS-mode. A 520 Hz CAOS pixel FM rate is selected with a 1 second data acquisition time per pixel and the 65536 samples/sec DAC sampling rate gives a DSP FFT (Fast Fourier Transform) gain of 45.2 dB. The CAOS sampling zone per patch selected for the FM TDMA-1 mode is 225 (i.e., 15 x 15) CAOS pixels where each CAOS pixel contains 6 x 6 micromirrors. Given 3 patches are viewed in the FM TDMA-1 mode, the encoding time is 3 x 225 = 675 seconds. Table 2 indicated that two more patches are accurately recovered using the FM TDMA-1 mode leaving 4 patches for recovery. The signal value in the FM TDMA-1 mode is first measured using the FFT peak value for each CAOS pixel before computing the average FFT peak value for a sub-zone comprising of the 36 brightest CAOS pixels. Hence, the SNR for FM

TDMA-1 mode data is computed in the same way as for the CDMA mode.

To recover the remaining 4 patches, the FM TDMA-2 mode is used that engages a larger size CAOS pixel (i.e., 84 x 84 micromirrors) to produce a higher SNR during the per bit time photo-detection process so one can detect a higher DR, i.e., weaker light signal from the patch. Indeed this is the case where even the weakest 90 dB DR patch is recovered at an SNR=11. Hence all remaining 4 patches in the scene are recovered accurately. Given 4 patches were observed in the FM TDMA-2 mode, the total encoding time is 4 seconds. For the FM TDMA-2 mode, patch scaled irradiance signal values are given by the FFT peaks for each CAOS pixel while the noise floor is computed by taking the average of the FFT noise floor over 100 points on either side of the FFT peak. Another point to make with respect to Table 2 CAOS DR data for each patch is that the data is highly robust because all CDMA CAOS readings are also confirmed using the FM TDMA-1 mode as shown for comparison in Table 3.

Table 3. Shown are the designed and CDMA and FM TDMA-1 CAOS mode measured patch DR values upto 54 dB DR CDMA limit. Table highlights redundancy and robustness of the CAOS-mode irradiance data for test patches.

Design (dB)	CAOS CDMA Measured (dB)	CAOS FM TDMA-1 Measured (dB)	CAOS FM TDMA SNR
0	0	0	1758
6	4.19	4.09	1097
12	10.06	10.01	550
18	15.53	15.21	305
24	24.75	24.66	103
30	28.20	29.47	59
36	33.09	33.42	37.5
42	39.6	40.44	16.7
48	47.5	48.37	6.7
54	54.04	56.01	2.8

Table 2 shows that the measured CMOS-mode patch DR readings are robust only up to the 42 dB DR patch, highlighting the CMOS sensor's single snap shot failure to track the low contrast patches when DR exceeds 48 dB. Specifically, the CMOS sensor shows very poor contrast detection sensitivity at low light levels (Patches from 48 to 90 dB DR values) while manages robust contrast detection at the brighter light levels (Patches from 0 to 42 dB DR values). On the contrary, the CAOS modes robustly recover all the 16 white light patch DR values with accuracy over the full 90 dB range. CAOS possesses a variety of operational modes that are suited from very low light levels to very bright light levels with adequate SNR control for robust, i.e., true irradiance recovery allowing low contrast HDR imaging over the full 90 dB test DR.

Fig.5 shows the Table 2 data plots that provides information on the CRF for the two modes of the CAOS smart camera. CMOS sensor data plot for the deployed experimental CMOS sensor shows an approximately linear response in the brighter light region for input irradiance DR range variation of 42.9 dB. Using curve fitting

computational methods seeking a slope nearest 1 over for the acquired data in the brighter light region, a CMOS-mode CRF slope of 1.05 is determined with a $\pm 3.34\%$ upper/lower bound with 95% confidence of fit. The ideal camera linear response slope of 1 indicates that an α dB DR variation in target contrast shows up as an α dB variation in sensor output current/voltage signal, thus producing an output signal without compression or expansion in order to represent the true gray-scale (i.e., contrast variation) of the observed image.

Note that the CMOS sensor data indicates a highly non-linear response in the weaker light region over a 42 dB DR variation range starting from slightly below the 48 dB DR data point position to the 90 dB extremely weak light irradiance level data point position. Hence low contrast image detection by the CMOS-mode of the CAOS smart camera is only possible due to the linear CMOS-mode response in the brighter light region while low contrast image detection fails because of the non-linear CMOS-mode response in the weaker light region.

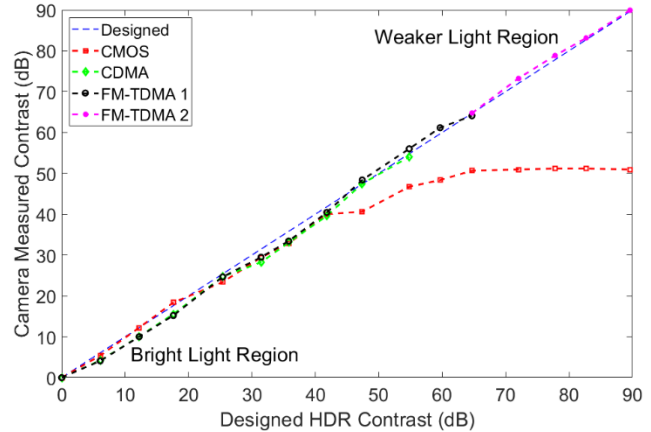


Figure 5. Designed target scaled input 16 irradiance values plotted versus camera modes measured patch DR values using Table 2 data. These plots provide the CMOS-mode and the CAOS-mode CRFs for the smart camera.

On the contrary, the CAOS-mode camera response is highly linear over the entire 90 dB DR irradiance range. The FM TDMA CAOS-mode data using curve fitting computational methods over the full 90 dB DR in the brightest to weakest light region gives a camera response slope of 0.9978 with a $\pm 3.2\%$ upper/lower bound with 95% confidence of fit. These results point to both the high linearity of the CAOS-mode camera response as well as the trueness (i.e., no sensor output compression/expansion) of the CAOS-mode observed scene recovery needed for robust low contrast image detection over an EDR.

The Fig.5 irradiance data requires special processing to enable 2-D or image format viewing in this paper so low contrast image recovery can be observed. As shown in Fig.6 (a), to display the CMOS-mode provided irradiance readings over a near 51 dB DR, the irradiance values are displayed over a 60 dB colour coded range. Note that the 4 patches in the leftmost column and the top most patch in the 2nd column from left in the Fig.6(a) image, which all have near 50 dB CMOS-mode provided DR readings show up looking the same, highlighting the fact that the CMOS sensor was unable to recover low contrast patches in the scene for the weaker light levels between the 66 dB and 90 dB DR range. In addition, the scaled irradiance readings provided by the CMOS-mode between 48 dB and 66 dB input DR values show up compressed (e.g., a 60 dB input DR is recovered as a 48.34 dB value) and give erroneous inter-patch scaled irradiance data for image reconstruction. Nevertheless, the CMOS-mode Fig.6 (a) image indicates the contours of all 16 patches in the 90 dB HDR target indicating the weak light sensing nature of CMOS sensor technology, i.e., low photon counts per second still register electron generation with an SNR slightly over 1 and adequate for binary state

light spatial registration. Knowing this spatial contour information for the 16 patches allows the CAOS-mode to implement a precision and guided HDR imaging operation that produced the Table 2 data. Using the Fig.6 (a) provided contour information, Fig.6 (b) shows an updated scene image where the CAOS readings per patch from Table 2 are used to provide the true scene irradiance values, shown over a 90 dB colour coded scale. Indeed, Fig.6 (b) shows low 6 dB step contrast recovery over all 16 patches of the observed target, a feature of the CAOS-mode when combined with the CMOS-mode of the presented dual-mode CAOS smart camera.

An important point to clarify regarding CMOS/CCD/FPA camera operations versus CAOS camera operations is the difference between the CMOS/CCD/FPA camera photo-sensor pixel exposure time (or pixel photo-electron integration time) versus the CAOS camera point detector response time. Specifically, the CAOS camera point PDs take a specific time to produce a steady state voltage response to the incident light. This response time depends on the electrical bandwidth of the point PD which can include a built-in transimpedance (i.e., photo-current to voltage) variable gain amplifier. For example, the point PD response time for typical commercial Thorlabs point PD ranges from a fast 100 ns for a photo-diode point detector to a slower 50 μ s for a PMT point detector. Thus, the CAOS mode on-off light modulation bit time should always exceed the response time of the point PD so that the DAC has adequate steady state voltage levels to sample in the photo-generated CAOS encoded signal.

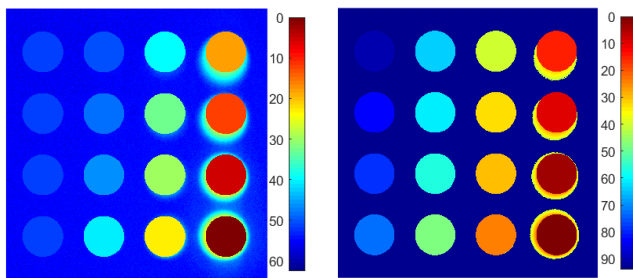


Figure 6. (a) Left Figure: CMOS-mode image adjusted for viewing. (b) Right Figure: CAOS calibrated true CMOS image.

CMOS Sensor Camera Characterization

As experimentally verified in the previous section, the performance of the designed CAOS smart camera also depends on the experimental performance of the deployed CMOS sensor. The experiments described earlier used a Thorlabs (USA) Model CS2100-M 2.1 Mpixel Quantalux monochrome silicon CMOS sensor with a 16-bit output and data sheet specified up-to 87 dB HDR, < 1 electron (e-) mean read noise (< 1.5 e- RMS noise), and \geq 23 K-electrons pixel full well capacity. Table 2 indeed shows that this s-CMOS sensor is able to register seeing a 87 dB HDR target, i.e., provides a sensor signal output just above the noise floor (so SNR>1). Nevertheless, Table 2 also points out that the CMOS sensor provided output signals register the seen target as a 51 dB DR target, providing erroneous image data information about the true target. The Thorlabs data sheet predicts an up-to 87 dB HDR detection. Here-in lies a disconnect with what the data sheet offers versus what is actually observed experimentally by the s-CMOS sensor camera when looking at a real HDR calibrated target. Furthermore, the CMOS sensor output signals across the full HDR are not scaled to match the individual target patch optical attenuations, thus failing low contrast recovery in the > 42 dB to 90 dB region

An important point to note is that current commercial CMOS image sensors and cameras such as available from European manufacturers (e.g., Photonfocus, Switzerland) are providing equipment validation data and performance specification sheets based on the 2016 European Machine Vision Association (EMVA) 1288 Release 3.1 standards [22]. These EMVA standards use several

critical assumptions to represent an ideal sensor and camera. For example, the sensor and camera are assumed to be linear over its operational range. The EMVA 1288 standards stress that the real sensor-based camera's deviation from the ideal sensor and camera operations must be small, otherwise the standards are not an accurate representation of the real camera system performance and the camera parameters derived can be "too uncertain and may even render meaningless". Given real CMOS sensors are based on the physics of photon and electron interactions in sensor optics and electronics, the sensor inherently has some non-linear operational regimes within a sensor's full dynamic range. Thus, the EMVA 1288 standards for best equipment representations should be used within a select narrower operational range that has been experimentally verified using custom calibration targets, such as presented in this paper. Our experiments with the Photonfocus lin-log CMOS sensor camera Model MV1-D1312 with specifications of 12-bits, 1312 x 1082 pixels, 8 micron side square pixel, indeed verify these EMVA 1288 standard issues where the specified 60 dB linear-only DR mode and 0-to-60 linear combined with specified 60 dB to 120 dB log-mode cannot accurately measure the target patch DR values for a presented 94 dB HDR low contrast multi-patch target. Specifically, with the Photonfocus CMOS camera set in its linear-only mode with exposure time set to 0.85 ms so brightest patch is below saturation, the imager does register the presence of the HDR 60 dB target patch, but the CMOS sensor output signals indicate an erroneous maximum 23 dB DR and with incorrect output readings for the individual patches weaker than the 14 dB patch.

With the camera next set to its higher 120 dB lin-log mode with exposure time increased to 22 ms to recover weaker light level target patches, a sensor output signal is registered experimentally up-to the 84 dB patch level and this signal compared to the brightest patch level indicates a near 23 dB DR due to the strong log compression in operation. In this case, sensor outputs do not match the patch levels over the entire 84 dB recovered range. This data highlights that the true target image DR data is not recovered. In addition, the 6 dB contrast steps between target patches is also not recovered with this sensor. Photonfocus data sheet for this camera [23] operating in the 60 dB linear mode specifies a minimum detectable photo-detected signal of 108.54 e- and saturation quantum well capacity of 83954 e- which computes to a data sheet stated 57.8 dB camera DR that matches the 60 dB linear DR limit.

It is important to note that the minimum detectable photo-detected signal is computed using an SNR formula with SNR=1 and using a measured output dark current parameter. This formula in the EMVA 1288 standard requires that the assumptions for the ideal sensor are met. Again, here-in lies a disconnect with what the data sheet predicts as camera performance and what is observed experimentally using a non-ideal CMOS sensor camera.

Conclusion

For the first time, successfully experimentally demonstrated is the low contrast CAOS imaging for a 90 dB HDR calibrated 16 patches test target where each patch pair has a 2:1 relative irradiance step, i.e., a 6 dB DR difference. Also shown are the limitations in low contrast HDR imaging of a deployed 87 dB HDR commercial CMOS sensor that achieved low contrast image detection over the brighter light region up-to a 42 dB DR of the test target. Scaled irradiance data for both the CMOS-mode and CAOS-mode of the CAOS smart camera are provided that highlight the very good linearity of the CAOS-mode over the target 90 dB HDR while the CMOS-mode behaves with a linear operation in the brighter light region with a non-linear response for mid-to-weak light regions.

Also highlighted for a specific CMOS sensor is the disconnect between EMVA 1288 standard predicted commercial CMOS sensor camera performance specifications and the experimentally measured HDR target camera data as EMVA standards assume that real CMOS sensors are near ideal sensors. With the initial demonstrated capabilities in this paper, the CAOS smart camera can potentially impact critical low contrast imaging applications within HDR scenes

[24] and potential 180 dB EDR scenes, in particular where camera data reliability are key requirements such as snow/desert/sea/air search and rescue, automotive vision, industrial vision safety systems (e.g., night vision for aircraft/ship/locomotive landing/docking) [25] as well as cancer detection [26].

To conclude, page 27 of the excellent HDR book by J. J. McCann and A. Rizzi [20] published in 2012 states: “Despite all the remarkable accomplishments, we cannot capture and reproduce the light in the world exactly.” In the spirit of AC and DC electric currents that light up the world, perhaps too can the CAOS smart camera bring us closer to achieving the HDR book’s stated goal by using AC photo-detected signal (i.e., CAOS) plus DC photo-detected signal (i.e., CMOS/CCD/FPA sensor) light capture and processing.

References

- [1] E. Reinhard, G. Ward, S. Pattanaik, and P. Debevec, *High Dynamic Range Imaging: Acquisition, Display, and Image-based Lighting*, Elsevier Morgan Kaufmann Publisher, 2005.
- [2] E. R. Fossum, S. Mendis, and S. E. Kemeny, “Active pixel sensor with intra-pixel charge transfer,” U.S. Patent 5471515, Nov. 28, 1995.
- [3] Y. Chen, X. Wang, A. J. Mierop, and A. J. P. Theuwissen, “A CMOS image sensor with in-pixel buried-channel source follower and optimized row selector,” *IEEE Trans. Electron Devices*, vol. 56, no. 11, pp. 2390–2397, Nov. 2009.
- [4] A. Boukhayma, A. Peizerat, and C. Enz, “Temporal Readout Noise Analysis and Reduction Techniques for Low-Light CMOS Image Sensors,” *IEEE Transactions on Electron Devices*, Vol. 63, No. 1, pp.72-78, January 2016.
- [5] I. Takayanagi, N. Yoshimura, K. Mori, S. Tanaka, S. Matsuo, H. Abe, N. Yasuda, K. Ishikawa, S. Okura, S. Ohsawa, T. Otaka, “An 87 dB single exposure dynamic range CMOS image sensor with a 3.0 μm triple conversion gain pixel,” *Proceedings of the International Image Sensor Workshop*, Vol.30, Hiroshima, Japan, 2017.
- [6] S. Cui, Z. Li, C. Wang, X. Yang, X. Wang, and Y. Chang, “A Charge Compensation Phototransistor for High-Dynamic-Range CMOS Image Sensors,” *IEEE Transactions on Electron Devices*, Vol. 65, No. 7, pp.2932-2938, 2018.
- [7] A. Tournier, F. Roy, Y. Cazaux, F. Lalanne, P. Malinge, M. McDonald, G. Monnot, and N. Roux, “A HDR 98 dB 3.2 μm Charge Domain Global Shutter CMOS Image Sensor,” *IEEE International Electron Devices Meeting (IEDM)*, pp. 10-4, 2018.
- [8] M. F. Tompsett, “Charge transfer imaging devices,” U.S. Patent 4085456, April 18, 1978.
- [9] T. Yamada, “CCD image sensors,” *Image Sensors & Signal Processing for Digital Still Cameras*, pp. 109-156. CRC press, 2017.
- [10] X. Li, H. Gong, J. Fang, H. Tang, S. Huang, T. Li, and Z. Huang, “The development of InGaAs short wavelength infrared focal plane arrays with high performance,” *Infrared Physics & Technology*, Vol.80, pp.112-119, 2017.
- [11] A. Spivak, A. Belenky, A. Fish, and O. Yadid-Pecht, “Wide-dynamic-range CMOS image sensors—comparative performance analysis,” *IEEE Transactions on Electron Devices*, Vol. 56, no. 11 2446-2461, 2009.
- [12] N. A. Riza and M. A. Mazhar, “177 dB Linear Dynamic Range Pixels of Interest DSLR CAOS Camera,” *IEEE Photonics Journal*, Volume 11, Number 2, April 2, 2019.
- [13] N. A. Riza, CAOS: Coded Access Optical Sensor (CAOS), USA Patent 10,356,392 B2, July 16, 2019.
- [14] N. A. Riza, M. J. Amin, J. P. La Torre, “Coded Access Optical Sensor CAOS Imager,” *J. Euro. Opt. Soc. (JEOS:RP)*. vol. 10, Apr. 2015.
- [15] N. A. Riza, “The CAOS Camera Platform – Ushering in a Paradigm Change in Extreme Dynamic Range Imager Design,” *TI Conference on DMD Technologies and Applications, SPIE OPTO*, Vol. 10117, Photonics West, Jan. 30, 2017.
- [16] N. A. Riza, “CAOS Camera Technology – Empowering Laser Metrology,” *Invited paper, European Optical Society Biennial Meeting, Conference on Frontiers in Optical Metrology*, Delft, Netherlands, Oct.8-12, 2018.
- [17] F. Farzaneh, A. Fotowat, M. Kamarei, A. Nikoofard, and M. Elmi, *Introduction to Wireless Communication Circuits*, River Publishers (Gistrup, Denmark and Delft, Netherlands), 2018.
- [18] N. A. Riza and M. A. Mazhar, “Laser Beam Imaging via Multiple Mode Operations of the Extreme Dynamic Range CAOS camera,” *Appl. Opt.*, vol. 57, no. 22, 1 August 2018.
- [19] 2:1 (or 6 dB) Contrast Patch Target Pairs-based HDR Contrast Resolution Chart, Imatest LLC, Boulder, USA.
- [20] J. J. McCann and A. Rizzi, *The Art and Science of HDR Imaging*. Vol. 26, John Wiley & Sons, 2012.
- [21] N. A. Riza and N. Ashraf, “Calibration Empowered Minimalistic Multi-Exposure Image Processing Technique for Camera Linear Dynamic Range Extension,” *paper in the IS & T Electronic Imaging Conference Proc.*, Burlingame, California, USA, Jan.26-30, 2020.
- [22] Standard for Characterization of Image Sensors and Cameras, European Machine Vision Association (EMVA) 1288 Release 3.1 standards, Dec. 30, 2016.
- [23] EMVA 1288 Data Sheet m00012, Photonfocus AG Switzerland, MV1-D1312-160-CL-12, 19589, 05 Oct.. 2016.
- [24] H. Singh, J. Adams, D. Mindell, and B. Foley, “Imaging underwater for archaeology,” *Journal of Field Archaeology*, Vol. 27, no. 3, 319-328, 2000.
- [25] L. Greenemeier, “Land and See: Infrared and 3-D Vision Systems Combine to Help Pilots Avoid Crash Landings.” *Scientific American*, February 8, 2012.
- [26] J. Schmidbauer, M. Remzi, T. Klatte, M. Waldert, J. Mauermann, M. Susani, and M. Marberger, “Fluorescence cystoscopy with high-resolution optical coherence tomography imaging as an adjunct reduces false-positive findings in the diagnosis of urothelial carcinoma of the bladder,” *European urology*, Vol. 56, no. 6, 914-919, 2009.

Author Biography

Nabeel A. Riza holds Masters (1985) & Ph.D. (1989) degrees in electrical engineering from Caltech. Since 2011, he holds the Chair Professorship in Electrical & Electronic Engineering at University College Cork, Ireland. His awards include the 2019 IS&T/OEA Edwin H. Land Medal, 2018 IET Achievement Medal, and 2001 ICO Prize. He is a Fellow of the US NAI, IEEE, OSA, EOS, SPIE, and Honorary Fellow Engineers Ireland Society. His research focus is applied optics and photonics.

Mohsin A. Mazhar holds a Bachelors (2016) degree in electrical engineering from LUMS School of Science & Engineering. He is a Ph.D. student under supervision by Prof. Nabeel Riza at the Photonics Info. Processing Systems Lab., University College Cork, Ireland.

JOIN US AT THE NEXT EI!

IS&T International Symposium on

Electronic Imaging

SCIENCE AND TECHNOLOGY

Imaging across applications . . . Where industry and academia meet!



- **SHORT COURSES • EXHIBITS • DEMONSTRATION SESSION • PLENARY TALKS •**
- **INTERACTIVE PAPER SESSION • SPECIAL EVENTS • TECHNICAL SESSIONS •**

www.electronicimaging.org

